Performance Characteristics of Hero's Turbine Using Hot Water as a Working Fluid*

Terushige FUJII**, Jun-ichi OHTA**, Koji AKAGAWA***,
Toshi NAKAMURA** and Hitoshi ASANO**

From the viewpoint of energy conservation and the development of new energy resources, it is important to utilize geothermal resources and waste heat from factories. Among energy conversion device, there is a radial outflow reaction turbine, i.e., Hero's turbine. Performance characteristics of Hero's turbine are analytically and experimentally clarified for flashing expansion of initially subcooled hot water. It is found that: (a) there is an optimum number of revolutions at which maximum turbine efficiency can be obtained; (b) Hero's turbine internal efficiency can be expressed as an algebraic equation and (c) nozzle loss accounts for almost 90% of the total turbine loss.

Key Words: Power Plant, Vapor Engine, Multiphase Flow, Total Flow Turbine, Turbine Efficiency, Loss Analysis

1. Introduction

From the viewpoint of energy conservation and the development of new energy resources, it is important to utilize geothermal resources and waste heat from factories. For this purpose, a total flow turbine has been proposed. The total flow turbine directly expands two-phase flows without throttling or separating them. Such a turbine system has the advantage of greater efficiency than other systems. The authors have investigated the performance of total flow turbine cycles[1),(2)].

As a total flow turbine, i.e., a two-phase expander, various types of expanders have been proposed, built and tested: for example, Hero's turbine[3)~(5)] (a radial outflow reaction turbine), an impulse turbine[6),(7)], a Lysholm engine[8),(9)] (a helical screw expander), a Wankel engine[10)], a Pelton wheel turbine[11)], and a Tesla turbine[12)], Steidel et al.[8)] and Taniguchi et al.[9)] designed and tested the Lysholm engine as a two-phase expander. The expansion ratio is limited owing to the displacement machine; thus, the range of power output is limited. Hijikata and Mori[10)] used a modified Wankel engine as a two-phase expander. The Wankel engine shows losses due to periodic admission of hot water and periodic exhaust of two-phase flow. Thus, a mechanism to minimize these losses is required. The impulse turbine is suitable for greater power capacity. Comfort[6)] and Sato et al.[7)] designed and tested the impulse turbine as a two-phase expander. The problem of erosion occurs when droplets hit the blades. The Tesla turbine is suitable for high rotational speed and is not affected by scale formation. Steidel and Weiss designed and tested the Tesla turbine[12)] and reported that maximum efficiency was 6.7%.

In this study, Hero's turbine has been chosen as a two-phase expander for both lower power output and flashing expansion of initially subcooled hot water. It consists of a simple mechanism and is not susceptible to the blade erosion problem. Efficiency characteristics of Hero's turbine were expressed as a simple

* Received 2nd September, 1991. Paper No. 90-0002 B
** Faculty of Engineering, Kobe University, 1-1 Rokkodai, Nada-ku, Kobe 657, Japan
*** Faculty of Science and Engineering, Ryukoku University, Setaoe, Otsu 520-21, Japan

algebraic equation by Comfort[6]. The equation, however, was not confirmed by experiments. House showed that Hero's turbine generated 130 kW at around 8 000 rpm[3]. In the authors' previous report[4], performance characteristics of Hero's turbine using an air-water two-phase mixture as a working fluid. In this paper, experimental and analytical results of performance characteristics of Hero's turbine are presented, for flashing expansion of initially subcooled hot water.

Nomenclature

C : Absolute velocity
C_T : Nozzle thrust coefficient
E_{in} : Energy of saturated hot water at turbine inlet
E_{out} : Output energy
h : Specific enthalpy
m : Mass flow rate
N : Number of revolutions
P : Pressure
T : Torque
T_{in} : Inlet temperature
U_e : Peripheral velocity
W : Relative velocity, $\vec{W}=\vec{U}_e+\vec{C}$ (See Fig. 2)
x : Steamquality
Z : Height
ΔT_{sub} : Inlet subcooling
η_t : Internal efficiency
Ω : U_e/V_{is}

Subscripts

e : Turbine outlet
g : Vapor
in : Turbine inlet
l : Liquid

2. Experimental Apparatus and Method

A schematic diagram of the experimental apparatus is shown in Fig. 1 and a cross section of Hero's turbine is shown in Fig. 2. Hero's turbine consists of a turbine chamber(4), two arm pipes(3), two nozzles (2) and a cylindrical chamber, which includes bearings and a mechanical seal(15). The radius at the nozzle exit is 312 mm and the angle, β, between the nozzle axis and the tangent of the circle ($R=312$ mm) at the nozzle exit is 30.1 degrees, as can be seen from Fig. 2. The cross section of the nozzle shows a sharp edge at the throat, a divergent angle of 6 degrees, convergent angle of 28 degrees, throat diameter of 2.5 mm and exit stream expansion ratio of 15.4. These parts were made of aluminum.

Tap water was softened by means of a water treatment, pressurized by a pump, and heated in a once through boiler(13). The hot water was then led to the cylindrical chamber through a separator which was attached to the boiler. Then, it was mixed with cooling water for the mechanical seal in the cylindrical chamber, led to the nozzles through the arm pipes, flashed in the nozzles, and discharged as two-phase flow jets. Reaction of the two-phase flow jet causes the turbine to rotate. Consequently, the turbine can generate shaft power.

The feedwater flow rate of the boiler was measured by an integrated flowmeter(12) installed upstream from the boiler, and the flow rate of the cooling water was measured by a rotameter (14) installed upstream from the mechanical seal. The flow rate of Hero's turbine is defined as the flow rate to the boiler plus that to the mechanical seal. Torque was measured by a torquemeter (8). Temperature and pressure at the turbine inlet were measured by a thermocouple and pressure transducer at the point where the hot water was mixed with the cooling water well (see Fig. 1). Rotational speed was measured by a noncontact-type revolution meter.

When Hero's turbine was externally driven with no loads by an electric servomotor(9), the product of the rotational speed and measured torque was taken to represent the losses in the gears, bearings, and mechanical seal. We term the losses a mechanical loss. The power output of Hero's turbine is a measured power output, i.e., the product of the rotational

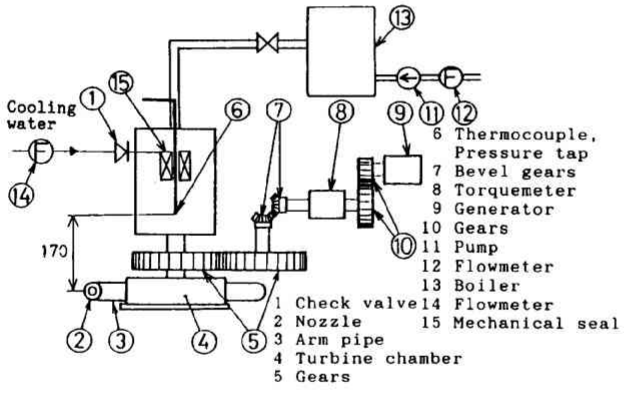

Fig. 1 Schematic diagram of experimental apparatus

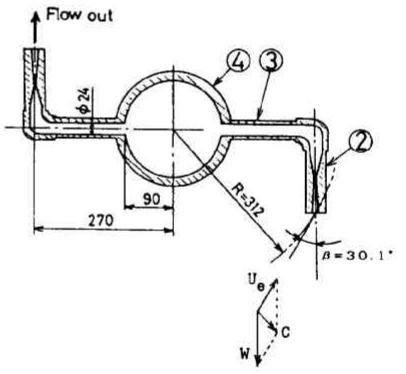

Fig. 2 Cross section of Hero's turbine

speed and torque $2\pi TN/60$, plus the measured mechanical loss.

The pressure and temperature at the inlet were set by adjusting the water flow rate and heat input to the boiler. To obtain a desired rotational speed, we adjusted the value of an electrical resistance attached to the servomotor. Experiments were carried out under the following conditions: inlet pressures ranged from 0.28 to 0.36 MPa, inlet temperatures ranged from 373 to 413 K (the inlet subcoolings of 31 to 4 K), and back pressure was maintained at 101.3 kPa by changing the flow rate.

3. Output, Internal Efficiency and Losses

3.1 Output and internal efficiency

In the case where the discharge angle for vapor is equal to that for liquid (see Fig. 2), the power output of Hero's turbine is defined as in Eq. (1), based on the separated flow model.

$$E_{out}=m\{x_e(W_{g,e}\cos\beta-U_e)+(1-x_e)(W_{l,e}\cos\beta-U_e)\}U_e. \quad (1)$$

The energy of subcooled hot water at the inlet can be expressed as

$$E_{in}=m\{h_{in}-h_e+\frac{1}{2}C_{in}^2+g(z_{in}-z_e)\}. \quad (2)$$

The turbine internal efficiency can also be defined as

$$\eta_i=\frac{E_{out}}{E_{in}}. \quad (3)$$

When flashing occurs in Hero's turbine, the relationships $0.5C_{in}^2\ll h_{in}-h_e$ and $g(Z_{in}-Z_e)\ll h_{in}-h_e$, in Eq. (2) are satisfied[**1]. Thus, E_{in}/m is approximately equal to the value of $h_{in}-h_e$ in Eq. (2), i.e., $0.5V_{is}^2$, where V_{is} is the ideal velocity of two-phase flow at the exit of Hero's turbine for the isentropic process at $N=0$ rpm. Therefore, the turbine internal efficiency can be expressed approximately as

$$\eta_i=\frac{x_e(W_{g,e}\cos\beta-U_e)U_e+(1-x_e)(W_{l,e}\cos\beta-U_e)U_e}{\frac{1}{2}V_{is}^2} \quad (4)$$

Since the hot water obtained energy of $0.5Ue^2$ due to the rotation, the theoretical relative velocity at the turbine exit W_{th} can be expressed as

$$W_{th}=\sqrt{U_e^2+V_{is}^2}. \quad (5)$$

The nozzle thrust coefficient is defined as the ratio of an actual thrust to a theoretical thrust using Eq. (5); thus, the nozzle thrust coefficient can be written as

$$C_T=\frac{x_eW_{g,e}+(1-x_e)W_{l,e}}{\sqrt{U_e^2+V_{is}^2}}. \quad (6)$$

Substituting Eq. (6) into Eq. (4) and replacing U_e/V_{is} with Ω, Eq. (4) can be rewritten as

$$\eta_i=2(C_T\cos\beta\sqrt{\Omega^2+1}-\Omega)\Omega. \quad (7)$$

In Eq. (7), loss due to the slip between vapor and liquid in the nozzle is contained in the value C_T. When the difference in discharge angles between vapor and liquid is small and loss between the turbine and nozzle inlets is negligible, it is seen from Eq. (7) that the efficiency of Hero's turbine is determined by the nozzle thrust coefficient C_T, dimensionless peripheral velocity Ω, and discharge angle β.

3.2 Analysis of losses

Losses in Hero's turbine can be divided into three types: (1) Energy loss in the passage between the turbine inlet and nozzle inlets is denoted as L_{ch1}. (2) Energy loss in the nozzle is denoted as a passage loss, L_{ch}. (3) Kinetic energy of the two-phase flow at the outlet of the turbine is denoted as an exit loss, L_e. L_{ch1} was measured using water with a temperature range of 278 to 283 K by the method described in Nakamura's study[13]. Since measured value of L_{ch1} in this method was maximum 3W and the ratio of L_{ch1} to E_{in} was less than 0.003[13], L_{ch1} was ignored in this loss analysis. Therefore, energy balance can be expressed as

$$E_{in}=E_{out}+L_{ch}+L_e. \quad (8)$$

The passage loss L_{ch} can be determined using nozzle efficiency. Nozzle efficiency η_N can not be measured directly. Therefore, it was estimated, based on an approximate relationship[**2] as

$$\eta_N\fallingdotseq C_T^2. \quad (9)$$

Since η_N was given using energy between the nozzle inlet and exit, and the passage loss was given using energy between the turbine inlet and outlet, the passage loss can be expressed as

$$L_{ch}=\left\{1-(U_e^2+V_{is}^2)\frac{C_T^2}{V_{is}^2}\right\}E_{in}. \quad (10)$$

The thrust coefficient can be estimated as follows: Thrust is defined as

$$F=m\{x_eW_{g,e}+(1-x_e)W_{l,e}\}. \quad (11)$$

Substituting Eq. (1) into Eq. (11) yields

$$F=\frac{E_{out}+mU_e^2}{U_e\cos\beta}. \quad (12)$$

Substituting Eqs. (12) and (11) into Eq. (6), the thrust coefficient can be rewritten as

$$C_T=\frac{(E_{out}+mU_e^2)/(mU_e\cos\beta)}{\sqrt{U_e^2+V_{is}^2}}, \quad (13)$$

where E_{in} was measured and L_{ch} was obtained by substituting measured values of E_{out}, m, U_e, and E_{in}

[**1] In this experimental condition, the kinematic energy of the hot water at the inlet was less than 0.04 % of the adiabatic heat drop. The potential energy between the measuring point and the turbine exit was less than 0.63 % of the adiabatic heat drop.

[**2] For a slip ratio of 10, the error of this approximation can be estimated at a maximum of 2.7% of the adiabatic heat drop. In this loss analysis, exit loss L_e includes the error of passage loss L_{ch} in Eq. (8).

into Eqs. (9), (10), and (13). The exit loss L_e was calculated by substituting L_{ch} and measured values of E_{in} and E_{out} into Eq.(8).

4. Experimental Results and Discussion

4.1 Output characteristics

4.1.1 Torque and power output Measured torque T is plotted against the rotational speed in Fig. 3. The measured torque is inversely proportional to the rotational speed for a constant flow rate, and decreases with increasing rotational speed. It can be seen that the measured torque increases with decreasing inlet subcooling ΔT_{sub} in the range below 11 K at constant rotational speed, but the inlet subcooling has little effect on the torque in the range above 14 K.

Measured power output E_{out} is plotted against the rotational speed with the inlet subcooling as the parameter in Fig. 4. The power output increases with rotational speed, but the output gradient, with respect to the rotational speed, becomes smaller as the rotational speed increases. The power output is varied from 16 to 40 W for inlet subcoolings of 3 to 14 K and from 10 to 17 W for subcoolings of 14 to 31 K. It can be seen that the effect of the inlet subcooling on the power output is similar to that on the torque.

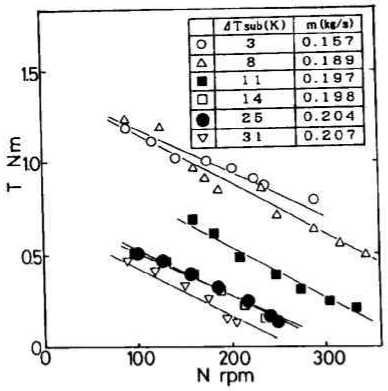

Fig. 3 Torque versus rotational speed

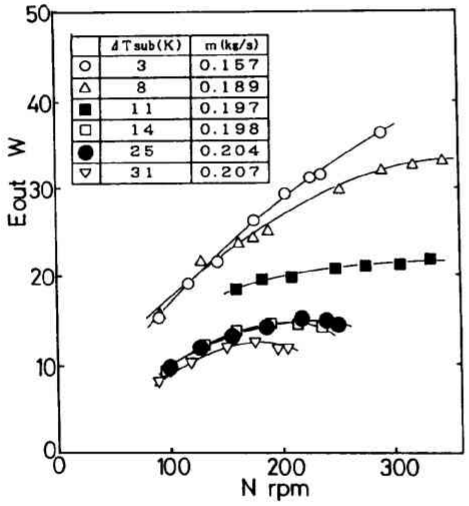

Fig. 4 Power output versus rotational speed

4.1.2 Turbine internal efficiency Measured efficiency η_i is plotted against the rotational speed with the inlet subcooling as the parameter in Fig. 5. In this figure, η_i is higher in the range of inlet subcoolings of 25 to 31 K, and lower in the range of inlet subcoolings of 3 to 11 K. It can be seen that the effect of the inlet subcooling on the efficiency is opposite to the effect on the power output. This is attributable to the fact that flashing occurs in the nozzles and thermal energy can be converted into power output in the range of inlet subcoolings of 3 to 11 K, but phase change does not occur in the nozzles to an extent sufficient to produce power output in range of inlet subcoolings of 25 to 31 K. Thus, it is important to design a nozzle which can fully convert thermal energy into kinetic energy of a two-phase flow for a given inlet subcooling and back pressure. As can be seen from the figure, there is an optimum rotational speed at which maximum efficiency can be obtained, except at an inlet subcooling of 3 K. The results do not attain maximum efficiency for the inlet subcooling at 3 K. The optimum number of revolutions increases with decreasing inlet subcooling.

Maximum efficiency $\eta_{i,max}$ is plotted against the turbine exit thermal equilibrium quality $x_{e,s}$ in Fig. 6. As $x_{e,s}$ increases to 0.035, $\eta_{i,max}$ decreases drastically. However, $\eta_{i,max}$ increases slightly at values above $x_{e,s}$ =0.035. This is considered to be due to the fact that the state in the nozzle changes from a single phase flow (liquid) to a two-phase flow with increasing $x_{e,s}$ to 0.035, and that, as $x_{e,s}$ becomes larger than 0.035, droplets in the nozzle are more accelerated.

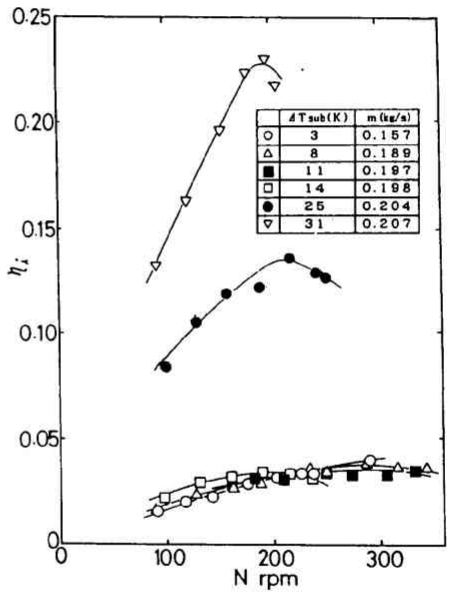

Fig. 5 Internal efficiency versus rotational speed

4.1.3 Nozzle thrust coefficient The thrust coefficient of the nozzle attached to the turbine was measured in a stationary state ($N=0$ rpm). The experimental apparatus and methods have already been reported in the authors' previous paper[14]. The measured value of the static thrust coefficient was 0.55 for an inlet pressure of 0.3 MPa and subcooling of 14.4 K. The estimated thrust coefficients from Eq. (13) are plotted against the rotational speed with the inlet subcooling as the parameter in Fig. 7. It can be seen that the estimated thrust coefficients ($N=100$ to 250 rpm) are lower than the measured static thrust coefficient ($N=0$ rpm) for an inlet subcooling of 14 K. This phenomenon can be explained as follows: As rotational speed increases, droplets are deposited on the inner wall of the nozzle due to centrifugal force, and the kinetic energy of the droplets decreases. Thus, the results of the estimated thrust coefficient appears to be reasonable. The estimated thrust coefficient increases for inlet subcoolings of 25 K and 31 K, as expected in section 4.1.2. It can be seen that as the rotational speed increases, the estimated thrust coefficient decreases, as in Fig. 7. To achieve a highly efficient Hero's turbine, It is important to develop a nozzle which shows higher thrust coefficient at higher rotational speeds.

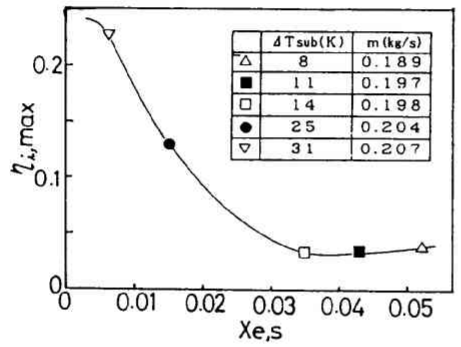

Fig. 6 Maximum internal efficiency versus exit thermal equilibrium quality

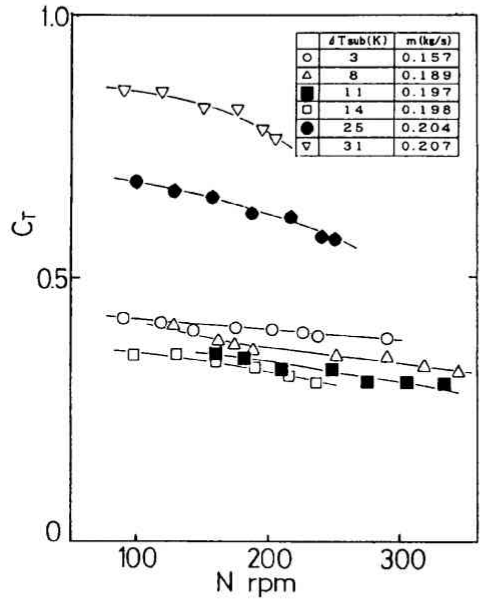

Fig. 7 Nozzle thrust coefficient

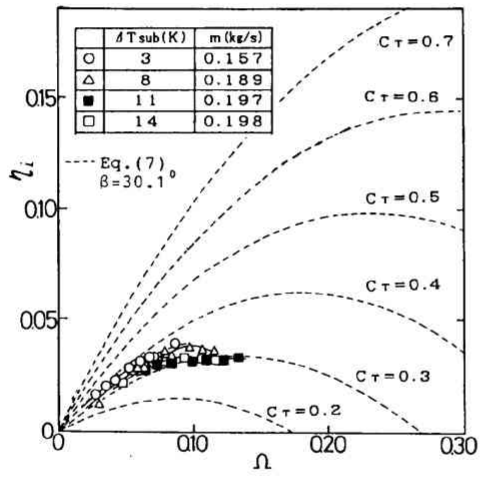

Fig. 8 Internal efficiency versus dimensionless rotational speed

4.1.4 Efficiency and dimensionless rotational speed The measured efficiency is plotted against the dimensionless rotational speed Ω as the symbols and calculated efficiency from Eq. (7) using $\beta=30.1$ degrees as a broken line in Fig. 8[**3]. As can be seen from this figure, the measured turbine efficiency agrees with the calculated turbine efficiency using the estimated thrust coefficient in Fig. 8. This indicates that the results of both the efficiency and thrust coefficient, calculated from Eqs. (13) and (7), are consistent with the measured results. Therefore, we can predict turbine efficiency from Eq. (7), if values of the nozzle thrust coefficient during rotation are known.

4.2 Loss analysis

Losses are normalized by the energy of the hot water at the inlet E_{in}. The results are plotted against the dimensionless rotational speed with the inlet subcooling as the parameter in Fig. 9, in the subcooling range of 3, 8 and 11 K. It can be seen that the passage loss ratio L_{ch}/E_{in} exit loss ratio L_e/E_{in} and power output ratio E_{out}/E_{in} are 0.82 to 0.91, 0.16 to 0.11, and 0.015 to 0.04, respectively. This loss analysis indicates that the passage loss, related to the nozzle efficiency, is dominant. This is attributable to the fact that the nozzles were not optimized for the back pressure and rotational speed. It is found that designing a higher

[**3] Measured data for inlet subcoolings of 25 and 35 K are excluded in Fig. 8, because it appears that flashing did not occur in the nozzles as described in section 4.1.2.

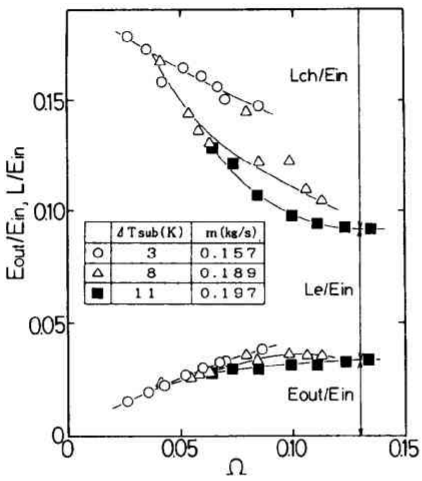

Fig. 9 Loss ratios and power output ratio versus dimensionless rotational speed

thrust coefficient nozzle taking into account back pressure and rotational speed is important for achieving a highly efficient turbine.

5. Conclusions

Performance characteristics of Hero's turbine are clarified, experimentally and analytically, for flashing expansion of initially subcooled hot water.

(a) There is an optimum rotational speed at which maximum turbine efficiency can be obtained.

(b) Hero's turbine efficiency can be expressed by an algebraic Eq. (7).

(c) Nozzle loss amounts to almost 90% of the total turbine loss.

Acknowledgments

The authors would like to express their thanks to the Japan Securities Scholarship Foundation for their financial support. Their acknowledgments are also extended to Mr. O. Morimoto for preparation of this paper.

References

(1) Akagawa, K., Fujii, T., Ohta, J. and Takagi, S., Cycle Performance of Total Flow Turbine Systems (1st Report, Utilization of Saturated Hot Water), Trans. Jpn. Soc. Mech. Eng., (in Japanese), Vol. 52, No. 480, B(1986), p. 3052.

(2) Akagawa, K., Fujii, T., Ohta, J. and Takagi, S., Cycle Performance of Total Flow Turbine Systems (2nd Report, Utilization of Wet Steam), Trans. Jpn. Soc. Mech. Eng., (in Japanese), Vol. 54, No. 502, B(1988), p. 1509.

(3) House, P.A., Performance Tests of the Radial Outflow Reaction Turbine for Geothermal Applications, UCID-17902,(1978).

(4) Akagawa, K., Fujii, T., Takagi, S., Takeda, M. and Tsuji, K., Performance of Hero's Turbine Using Two-Phase Mixtures as Working Fluid (Experimental Results in an Air-Water Two-Phase System), Bull. JSME, Vol. 27, No. 234(1984), p. 2795.

(5) Takagi, S., A Study of Gas-Liquid Two-Phase Flow Turbine, Doctor Thesis(in Japanese), Kobe University,(1984).

(6) Comfort, W.J., The design and Evaluation of a Two-Phase Flow Turbine for Low Quality Steam -Water Mixtures, UCRL-52281,(1977).

(7) Sato, S., Kakihara, K. and Sakamoto, Y., An Experimental Study on the Efficiency of Very Low Quality Two-Phase Flow Turbine, Proc. of ASME/JSME Thermal Engineering Conference, (1983), p.207.

(8) Steidel, R.F., Weiss, H. and Flower, J.E., Performance Characteristics Lysholm Engine as Tested for Geothermal Power Applications in the Imperial Valley, Trans. ASME, J. Engineering for Power, Vol. 104, No. 1 (1982), p. 231.

(9) Taniguchi, H., Kudo, K, Giedt, W.E., Park, I. and Kumazawa, S., Analytical and Experimental Investigation of Two-Phase Flow Screw Expander for Power Generation, Trans. ASME, J. Eng. Gas Turbines Power, Vol. 110, No. 4 (1988), p. 628.

(10) Hijikata, K. and Mori, Y., Fundamental Performance Two-Phase Flow Rotary Expander, Trans. Jpn. Soc. Mech. Eng., (in Japanese) Vol. 48, No. 425, B (1982), p. 160.

(11) Akagawa, K. and Asano, Y., Performance of Pelton-Type Turbine Driven by Gas-Liquid Two -Phase Flow, Bull. JSME, Vol. 29, No. 247(1986), p. 106.

(12) Steidel, R. and Weiss, H., Performance Test of a Bladeless Turbine for Geothermal Applications, UCID-17068,(1976)

(13) Nakamura, T., A Study of the Characteristics of Hero's Turbine Using a One-Component Two-Phase Mixture, Master Thesis, (in Japanese) Kobe University, (1987)

(14) Akagawa, K., Fujii, T., Ohta, J., Inoue, K., and Taniguchi, K., Performance Characteristics of Convergent-Divergent Nozzles for Subcooled Hot Water, JSME Int. J., Ser.II, Vol. 31, No. 4 (1988), p. 718.